Molecular Dynamics Simulations of Li- and Na-Nafion Membranes

Daniel Brandell[*,a], Alar Ainla[b], Anti Liivat[a], Alvo Aabloo[b]

[a]Department of Materials Chemistry, Ångström Laboratory, Uppsala University, Box 538,
SE-75121 Uppsala, Sweden.
[b]Institute of Technology, Tartu University, Nooruse 1, 504 11, Tartu, Estonia.

ABSTRACT

Molecular Dynamics (MD) techniques have been used to study the structure and dynamics of hydrated Li- and Na-Nafion membranes. The membranes were generated using a Monte Carlo-approach for Nafion 117 oligomers of $M_w = 1100$ and with water contents of 7.5 and 20 % by weight, equivalent to 5 and 15 water molecules per sulfonate group, respectively. After equilibration, local structural properties and dynamical features such as coordination, cluster stability, solvation and ion conductivity were studied. In a comparison between the two cationic systems, it is shown that the Na-Nafion system is more sensitive than Li-Nafion to the level of hydration, and also show higher ion conductivity. The ionic conductivity is shown to increase with higher level of hydration.

Keywords: Artificial muscles, Ionomeric Polymer-Metal Composite, Nafion, Molecular Dynamics, cation-sulphonate group interactions, water-cation coordination, ion conductivity.

1. INTRODUCTION

Electroactive polymers (EAPs) are polymer materials that change their shape or size in response to electrical stimuli. This feature makes this class of materials to a good candidate in the field of biomimetics, since it mimics the behavior of biological muscles. EAPs which also inhibit properties similar to biological materials in terms of force, strain and speed are attractive for creating artificial muscles used in biologically inspired robots [1].

There are many types of electroactive polymers with various properties and with a various type of reaction to the electrical stimuli. Generally, EAP materials can be divided into two major groups: electronic and ionic EAPs. Ionic polymers have the advantage to operate at much lower applied electric fields than electronic EAPs. Among the most commonly used ionic EAP systems are the ionomeric polymer-metal composites (IPMCs), consisting of a ~200 μm thick ionomer membrane plated with metal (typically Pt or Au). The material exhibits a bending motion when a potential of 1-5 V is applied over the metal surfaces [2].

The ionomer membranes used in IPMCs are typically hydrated fluorinated polymers, of which Nafion is the archetype material. During material fabrication the protons connected to the terminal groups of the Nafion side-chains are replaced with metal cations. It is the movement of the cations towards the metal cathode due to the applied field which causes the bending motion (toward the anode) of the material. To increase the strength and speed of the material's response to stimuli, it is vital to increase the ionic conductivity in the membrane, and it is therefore an ultimate task for the research society [3].

The motion of the ions give rise to two boundary layers close to the metal surfaces of the IPMCs: An anode boundary layer depleted of cations, and a cathode boundary layer with cations in excess. There are then several mechanisms which lead to the characteristics of the bending motion in the IPMCs: changes in stiffness in the boundary layers, increased electrostatic repulsion between the anions in the anode boundary layer and the cations in the cathode boundary layers, reorientation of water molecules, a drag of water molecules by the ion migration, and a following change in osmotic pressure [4].

---

[*] Daniel.Brandell@mkem.uu.se; phone +46-18-4713701; fax +46-18-513548; www.mkem.uu.se

Nafion is a poly(tetraflouroethylene) (PFTE; Teflon) polymer with perfluorovinyl side-chains terminated with -SO$_3$H groups (see Fig. 1), which is commonly used as a proton-exchange membrane in methanol fuel cells. The Teflon backbone ensures high chemical stability. Nafion easily absorbs water, which forms a channel network in the polymer matrix. The polymer itself then separates into hydrophobic (backbone) and hydrophilic (the terminal group of the side-chain) domains, where the sulphonate groups sticks out into the water channels, where they can bind to the cations [5].

$$- (CF_2-CF)-(CF_2-CF_2)_n -$$
$$|$$
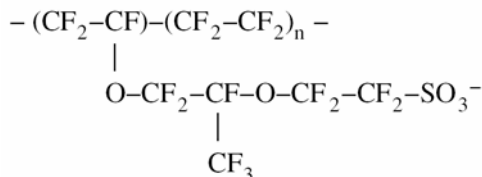$$O-CF_2-CF-O-CF_2-CF_2-SO_3^-$$
$$|$$
$$CF_3$$

Figure 1. The Nafion formula.

At the atomic and molecular level, there exist a number of competing interactions within the IPMC Nafion membrane. The electrostatic interaction between cations and the SO$_3^-$ groups is the major factor in the polymer-cation interaction, before electrostatic contributions from the polar groups on the side-chains and the Teflon backbone. The Nafion-cation interaction decreases with water content, since water dissolves both the cations and the SO$_3^-$ groups. However, the Nafion side-chains are hydrophobic, and therefore try to remain in the back-bone matrix, while the terminal SO$_3^-$ groups are being dragged into the channels. The solvation also leads to a high concentration of solvated cations in the middle of the water channels, where the ions themselves repel each other, and to a high concentration of SO$_3^-$ group at the channel surface, where electrostatic repulsion also occurs. To these interactions also come the energetically favorable interactions between water molecules [6].

It is difficult to obtain detailed experimental information on the processes and interactions mentioned above. Not least causes the inhomogeneousness of the morphological structure problems for studies with diffraction techniques. For this reason, atomic level simulations are valuable complements to experimental observations. Simulations and modeling can be used to study the network morphology, local structures and the crucial conduction mechanisms.

In this study we use Molecular Dynamics (MD) simulations to examine some structural and dynamical phenomena in the hydrophilic domains of the material. We have chosen to work with two of the most commonly used cations in IPMCs: Li$^+$ and Na$^+$. We have also chosen to study the effect of the water content, by adding 5 or 15 H$_2$O molecules per sulphonate group for both cation systems.

We present results from one of the first all-atom MD simulations of a Nafion-based IPMC membrane. Previous studies by Blake *et al.* [6] use a different force field and focuses solely on Na$^+$ as counter-ion to Nafion.

2. THE MD SIMULATIONS

In an MD simulation, atomic motion in a chemical system is modelled in classical mechanics terms by solving Newton's equations of motion simultaneously for all particles in an appropriately chosen periodic simulation box. This set of equations is solved by a computational algorithm and depends implicitly on the description of the forces acting between the particles. It was only recently, that the first fully atomistic MD simulations of Nafion were published [7].

2.1 The model
The Nafion formula can be seen in Fig. 1. In our model, we used 4 oligomers of Nafion, each containing 10 side-chains with a separation of 13 -CF$_2$- units, *i.e.* n = 6.5 in Fig. 1. This model closely resembles Nafion 117, one of the most studied Nafion versions. The water content was set to 5 or 15 molecules per sulphonate group, equivalent to 7.5 or 20 wt %, respectively (these are hereafter referred to as n = 5 and n = 15). The negatively charged sulfonic groups were completely saturated with counter-cations, *i.e.* the systems contained either 40 Li$^+$ or Na$^+$ ions.

The MD simulation box thus contained a total of 3368 or 4568 atoms depending on water content, and had cubic dimensions with *a* = 40.00 Å initially. The start structures were initially generated by the Monte Carlo polymer-

generation program *mcgen* [8], developed within our group. After polymer generation, water molecules and cations were inserted randomly in the box.

2.2 Force field

The intramolecular potential for Nafion, describing bending and torsional motion in the polymer chain, are here taken from Goddard *et al.* [7,9]. This set of potentials, developed from the DREIDING force field [10] and DFT B3LYP calculations on gas-phase perfluoromethane, has been used in several Nafion simulations and seem to reproduce the polymer-chain conformation satisfactorily. The flexible water potentials used in the simulations were taken from Levitt *et al.* [11], taking bending but not polarisation into account.

The Buckingham type potentials describing interactions between cations and water were taken from Spångberg *et al.* [12-14]. These potentials were developed from *ab initio* calculations and fitted to both bulk and ion cluster configurations, which is crucial for Nafion studies.

Any other type of intermolecular potential in the system was described by a combination of Buckingham or Lennard-Jones and electrostatic potentials:

$$U(r) = A\exp\left(-\frac{r}{B}\right) - \frac{C}{r^6} - \frac{D}{r^4} + \frac{q_1 q_2}{4\pi\varepsilon_0 r} \qquad \text{(Buckingham)}$$

$$U(r) = \frac{A}{r^{12}} - \frac{C}{r^6} + \frac{q_1 q_2}{4\pi\varepsilon_0 r} \qquad \text{(Lennard-Jones)}$$

where A, B, C and D are constants depending on the interacting atom-types. The values of the constants for different interactions within Nafion were taken from Goddard *et al.* [7], while other intermolecular potentials except water-water, water-cation and cation-cation could be obtained using Lorentz-Berthelot standard combination rules.

2.3 Simulation details

The MD simulations use periodic boundary conditions and an Ewald summation which treats the long-range electrostatic forces. The short-range cut-off used is 16 Å and the Verlet sphere used in the construction of the Verlet neighbour-list has a 0.5 Å radius. Both simulations consisted of an equilibration period of 100 ps at constant volume (NVT simulation), followed by 100 ps at constant pressure to relax the box dimensions. The temperature was then raised to 600 K for 100 ps, and then gradually lowered to 293 K by 6 K/ps, where the system showed equilibrium properties regarding volume and energy. The simulation continued for another 1,7 ns using a Nose-Hoover barostat. The sampling period for the analysis was the last 500 ps.

A multiple time-step technique was used, with a longer time-step of 1 fs for longer distances, and a shorter time-step of 0.2 fs inside a sphere of radius 6 Å. The simulations were performed under ambient conditions: 293 K and a pressure of 1 bar. The polymer MD simulation program used was DL_POLY [15].

3. RESULTS AND DISCUSSION

The equilibration process somewhat decreased the dimensions of the simulation box, with a more pronounced effect when the water content was lower. The final cubic dimensions were $a = 35.4$ Å (Li, low water content), $a = 37.65$ Å (Li, high water content), $a = 35.6$ Å (Na, low water content) or $a = 37.5$ Å (Na, high water content). The equilibration process also lead to a separation of the systems into their hydrophilic and hydrophobic parts; see Fig. 2 which shows the final snapshot of one of the MD boxes. The water is forming a matrix dissolving the ions and SO_3^- groups, thus making their concentration very high in these regions, in good agreement with what is found experimentally and in other simulations [6,7]. The water channel has a radius of approximately 8 Å for the systems with n = 5 and 12 Å for the systems with n = 15, irrespective of cation type.
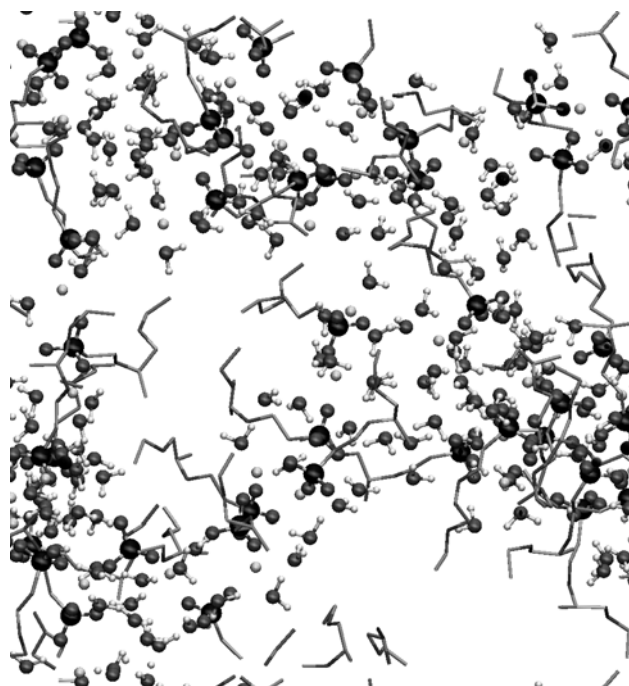
Figure 2. The simulation box of hydrated Li-Nafion, with 5 water molecules per sulphonate group. For clarity, the hydrophobic Teflon backbone of Nafion is only shown as empty space.

3.1 Na$^+$ and Li$^+$ coordination to H$_2$O

The Radial Distribution Function (RDF) $g_{AB}(r)$ shows the probability of finding an atom of type B at a distance of r Å from atom type B. The Coordination Number (CN) function shows the coordination number of B to A at the same distance. In Figure 3, the RDFs and CN functions for both types of ions towards water oxygen are shown (*i.e.* $g_{NaOW}(r)$ and $g_{LiOW}(r)$ and their respective CN functions) for both high and low level of hydration.
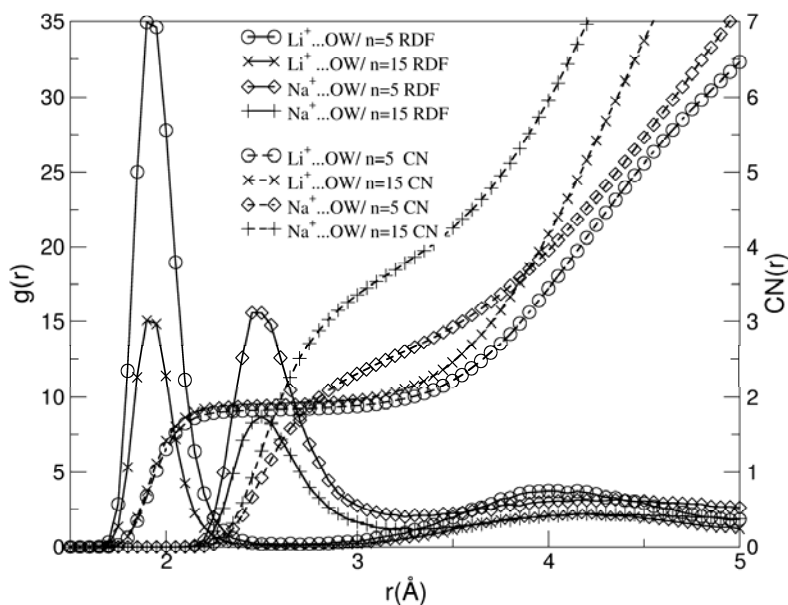

Figure 3. Na- and Li-OW radial distribution functions (RDF) and coordination number (CN) functions for hydrated Li- and Na-Nafion with 5 or 15 water molecules per sulphonate group.

All RDFs of both Li$^+$ and Na$^+$ has two distinct peaks, representing the inner and outer coordination sphere. For Li$^+$, the inner coordination sphere is located around 1.9 Å from the ion, while the outer is at 4.0 Å. For the larger Na$^+$ ions, the distances grow to 2.5 Å and 4.5 Å, respectively. These distances are normal for both atom types.

The Li$^+$ ions coordinate on average two different water molecules, indicating that there is a high coordination to the competing sulphonate groups. Interestingly, this average CN does not seem to change much when the level of hydration increases, indicating a comparably weak electrostatic interaction between Li$^+$ and H$_2$O. The Na$^+$ system responds differently to the level of hydration, with an expected increase in the water CN when the level of hydration increases.

There are clear signs of local dynamics of the water molecules surrounding the cations. Both cation types experience how the water molecules change their position around the ions, and even exchange place with other water molecules. An example of the latter can be seen in Fig. 4.
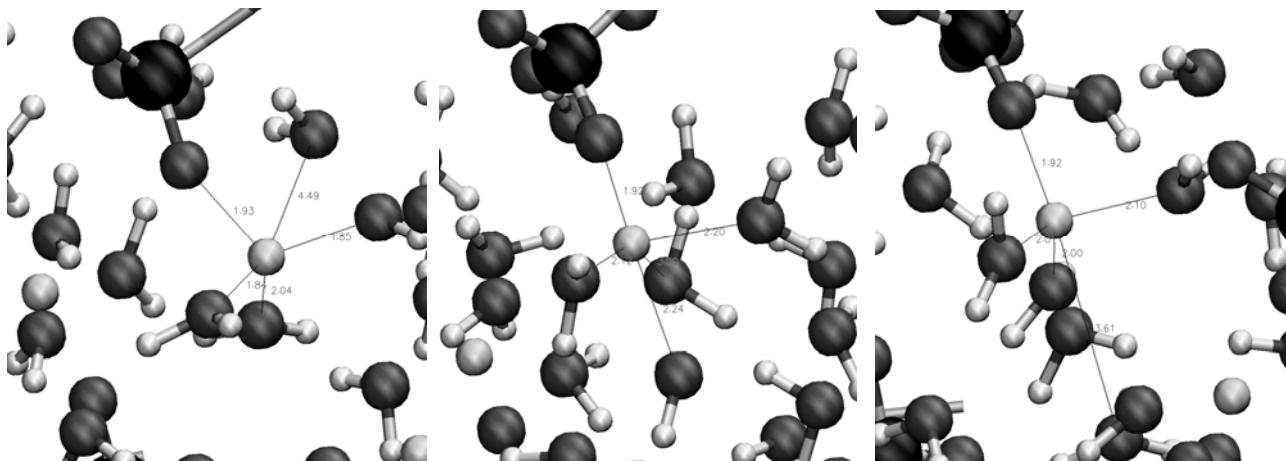

Figure 4. Two water molecules exchanging place around a Li$^+$ ion in Li-Nafion with 15 water molecules per sulphonate group. The exchange take place during 80 ps. The Li$^+$ atom is coordinated to an inner sphere of one sulphonate oxygen and three water molecules at the first and last snapshot shown, with an extra water molecule at a somewhat higher distance.
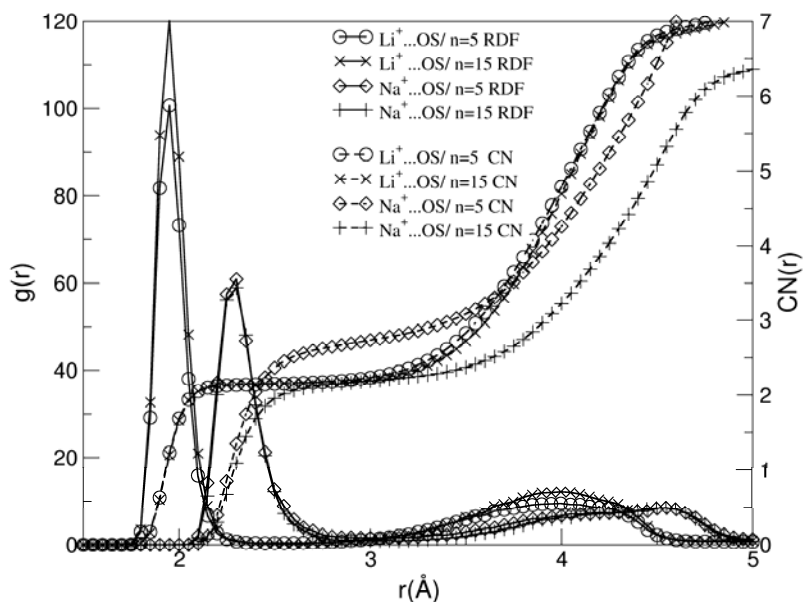

Figure 5. Na- and Li-OS radial distribution functions (RDF) and coordination number (CN) functions for hydrated Li- and Na-Nafion with 5 or 15 water molecules per sulphonate group.

3.2 Na$^+$ and Li$^+$ interactions with SO$_3^-$

Figure 5 shows the RDFs and CN functions for Na-OS and Li-OS for all simulated systems, describing the cation interactions with the SO$_3^-$ groups. All RDFs have two distinct peaks, one at a lower distance (around 2.0 Å for Li$^+$ and 2.3 Å for Na$^+$) and one at a higher (around 4.0 Å for Li$^+$ and 4.5 Å for Na$^+$). These peaks correspond to directly bound and dissociated ions, respectively, and the difference in distances again originates from the difference in ion radius.

For the Li-Nafion system, it is striking how small the difference is for the different level of hydration – higher water content does not seem to dissolve more ions; in fact the RDF peak at low distance is actually higher at higher water content. This indicates a very strong attraction between the Li$^+$ ions and the SO$_3^-$ groups. The same phenomena seem to occur also in the Na-Nafion system, although the CN to sulphonate oxygen here is higher at lower hydration level, indicating that some solvation occurs when the water content is increased.

3.3 The cation coordination spheres

The RDFs and CN functions for the cations to both water and sulphonate oxygens give the total picture of the coordination sphere around Li$^+$ and Na$^+$. Li$^+$ has a total CN of 4 at the distance 2-3 Å, coordinating two water molecules and two sulphonate oxygens. In most cases, these sulphonate oxygens come from the same SO$_3^-$ group. Most remarkable is that the situation does not change significantly with the level of hydration. Na$^+$, on the other hand, has more variations in its CNs, coordinating on average around 5-6 oxygen atoms. The high average CNs to sulphonate oxygen indicates that there are very few totally dissolved cations in all simulated systems.

This picture is also confirmed in the histograms showing the distribution of CN throughout the sampling periods (Fig. 6). Here it is clearly shown that Li$^+$ has a coordination number of 4 at almost every sampling point during the simulation, while the situation for Na$^+$ show more variety. There are also some Na$^+$ ions with high coordination numbers to water molecules, and which therefore are completely solvated in the water channel. The CN for both ions are rather common in many systems, and the distribution of the Na-clusters is also very similar to the one found by Blake *et al.* [6].
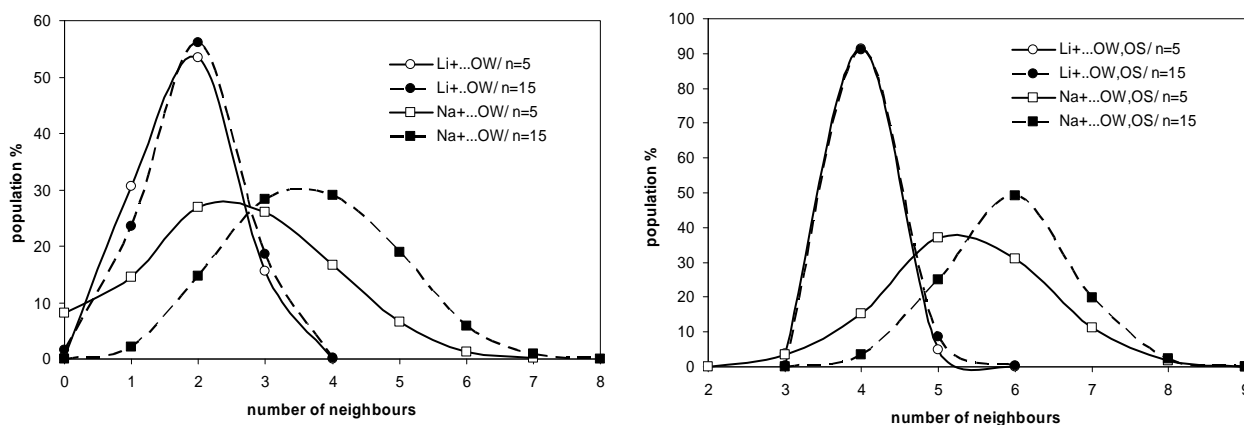

Figure 6. Histograms showing the number of H$_2$O molecules ("OW") and the total number of neighbors ("OW,OS") present in the first hydration shell around Li$^+$ and Na$^+$ as a percentage of the total number of sampled configurations. The lines are only present to guide the eye, and indicate no intermediate values.

By inspection of individual ions in the system, it is clear that the CN is changing during the simulation, thus indicating that there are many dynamical features taking place during the simulation. This also means that the individual cluster formations are far from stable. Fig. 7 shows the persistence of the first coordination sphere for both cations at a high hydration level, calculated according to Impey *et al* [16]. The sloping lines all represent individual cations in the simulations, and the downward slope indicates that the individual oxygen neighbors either vanish or are replaced by other. A decrease from 4 to 1 in the autocorrelation function during 200 ps thus means that only one of the initial four neighbors remain after this time. It is clear that the drop is more pronounced for Na$^+$ than for Li$^+$, thus showing that Li$^+$

forms more stable clusters. This again probably indicates the strong electrostatic bond between Li$^+$ and its SO$_3^-$. It is also significant that the stability of the clusters is decreasing when the water content gets higher.
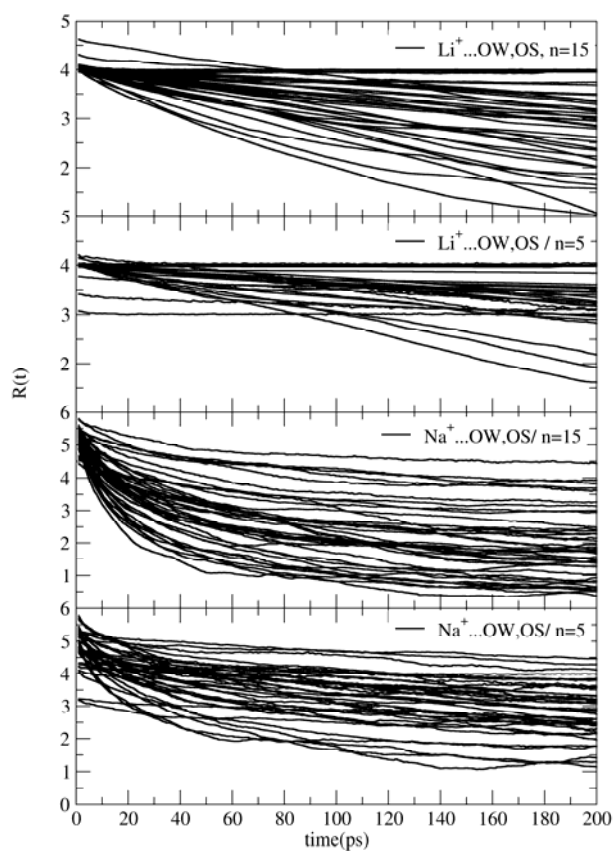

Figure 7. The persistence of the individual Li$^+$ and Na$^+$ coordination spheres in hydrated Nafion (5 or 15 water molecules per sulphonate group), shown as autocorrelation functions of the coordination numbers for the last 200 ps of the MD simulations. Note that the scales on the y-axes are different on different graphs.
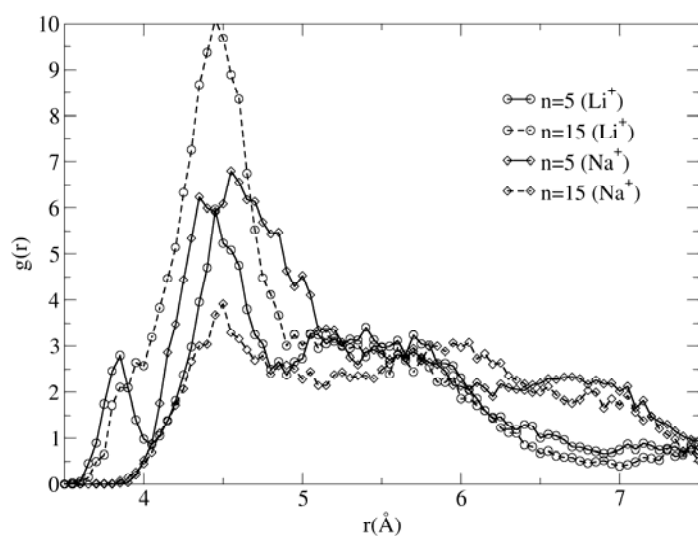

Figure 8. S-S radial distribution functions for Li- and Na-Nafion, with 5 or 15 water molecules per sulphonate group.

3.4 SO₃⁻ interactions

Fig. 8 show how the sulphur-sulphur (S-S) RDF $g_{SS}(r)$ depends on hydration level and cation type. It is an obvious that the interactions between the sulphonate groups varies with both cation type and the water content, although all curves peak around 4.5 Å. The trend is that the shorter S-S distances are preferred at lower level of hydration for both cation systems. This can be seen in Na-Nafion in the higher peak for lower distances. The reason for this is that the water content is so low, that some Na^+ ions have more than one SO_3^- neighbor, thus dragging the sulphonate groups toward each other. In Li-Nafion, the situation is analogous but more extreme, with a number of very close SO_3^- groups, less than 4 Å from each other, bridged by Li^+.

3.5 Cation migration

Figure 9 shows the Mean Square Displacement (MSD) plots for Li^+ and Na^+ for both studied levels of hydration. The diffusion coefficient (D) for the different ion types can be calculated from the slope of the MSD plots on the basis of:

$$D = \frac{1}{6Nt} \sum_{i=1}^{N} \left\langle x_i^2 \right\rangle + \left\langle y_i^2 \right\rangle + \left\langle z_i^2 \right\rangle$$
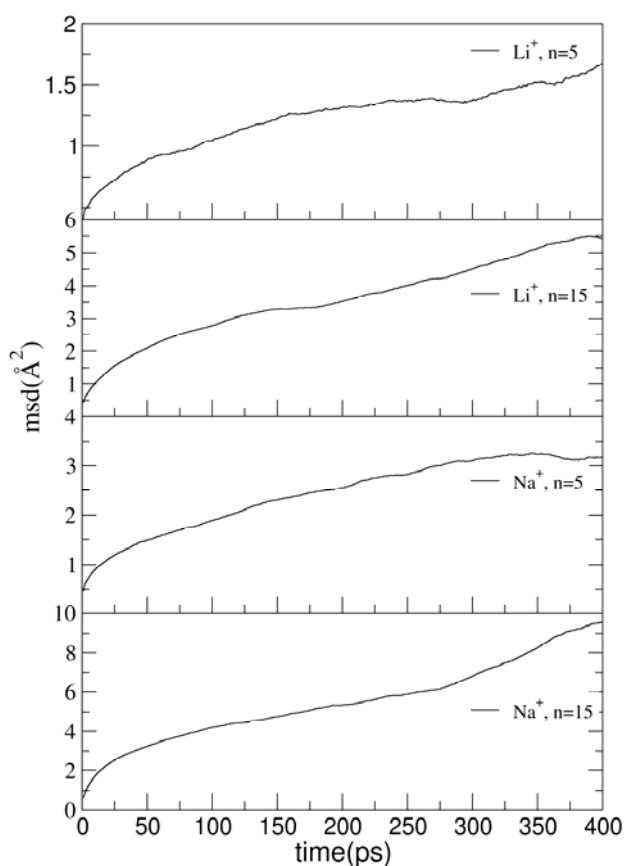

Figure 9. Mean Square Displacements for Li^+ and Na^+ in hydrated Nafion with 5 or 15 water molecules per sulphonate group. Note that the scale on the y-axis is different for different plots.

From the diffusion coefficient, the conductivity can be calculated by the Nernst-Einstein equation. The individual values of D and the corresponding conductivity values have not been calculated here due to the poor statistics. However, the graphs do indicate that the Na^+ systems experience much higher conductivity than the Li^+ cases, and that the higher level of water content also facilitates ion transport. The first phenomenon is not unexpected, considering the tight bonds between Li^+ and the immobilized SO_3^- groups discussed earlier. The coordination sphere around Na^+ is less stable, and

the ions can therefore diffuse more freely. The latter result is also consistent with the higher Na^+-H_2O coordination at higher level of hydration. It is interesting to see, however, that the level of hydration also has a clear effect on the Li^+ ion mobility although the overall coordination is independent of water content. This effect might be due to a different mobility mechanism, taking place while Li^+ is still coordinated to the SO_3^- groups.

4. CONCLUSIONS AND FUTURE WORK

The MD simulations indicate clearly that Na^+ has higher diffusion coefficient than Li^+ in these Nafion systems, and therefore might be a better candidate ion in IPMC membranes. However, the lack of stable water clusters around Na^+ might indicate that the higher Na^+ mobility does not lead to a corresponding higher water drag, and one can thus not make the conclusion that the final bending effect of the material will be more pronounced. The total water drag must be investigated further.

The simulation model presented here can undergo substantial improvements. Although some results was repeated from earlier simulations with other force fields [6] or showed agreement with experiment, there are still questions one can raise about the accuracy of the force field. That the Li^+ coordination is independent on the water concentration is an unexpected result, and might indicate that the attraction between Li^+ and SO_3^- is overestimated. The cation-sulphonate group potentials should be improved and fitted to quntum chemistry calculations or experimental data. Also the cation-water potentials can be developed further, to take the polarisability into account.

There is also a need to increase the simulation system size. Nafion has a highly complex and debated structure, and to get a good description of its morphology there is a need for a large repeating unit; maybe larger than our current box size. To simulate the system with an applied electric field, to better mimic its behavior in an IPMC application, would also be an improvement of the model.

5. ACKNOWLEDGEMENTS

REFERENCES

1. Y. Bar-Cohen, *Biomimetics – BiologicallyIinspired Technologies*, CRC, 2005.
2. Y. Bar-Cohen, *Electroactive Polymer (EAP) Actuators as Artificial Muscles - Reality, Potential and Challenges*, SPIE Press, 2001.
3. M. Shahinpoor, *Electrochim. Acta*, 48 (2003), 2343.
4. S. Nemat-Nasser, *J. Appl. Phys.*, **92** (2002) 2899.
5. K.A. Mauritz and R.B. Moore, *Chem. Rev.*, **104** (2004) 4245.
6. N.P. Blake, M.K. Petersen, G.A. Voth and H. Metiu, *J. Phys. Chem. B*, **109** (2005) 24244.
7. S.S. Jang, V. Molinero, T. Cagin and W. A. Goddard III, *J. Phys. Chem. B*, **108** (2004) 3149.
8. E. Soolo, J. Karo, H. Kasemägi, M. Kruusmaa and A. Aabloo, "Application of the Monte Carlo method for creation of initial models of EAP molecules for Molecular Dynamics simulation", Proceedings of the SPIE - The International Society for Optical Engineering, current edition. In print.
9. S.S. Jang, M. Blanco, W.A. Goddard III, G. Caldwell and R. Ross, *Macromolecules*, **36** (2003) 5331.
10. S.L. Mayo, B.D. Olafson and W.A. Goddard III, *J. Phys. Chem.*, **94** (1990) 8897.
11. M. Levitt, M. Hirshberg, R. Sharon, K.E. Laidig, V. Daggett, *J. Phys. Chem. B*, **101** (1997) 5051.
12. D. Spångberg, *J. Chem. Phys.*, **120** (2004), 4829.
13. D. Spångberg, *J. Chem. Phys.*, **119** (2003) 7263.
14. D. Spångberg, *Cation Solvation in Water and Acetonitrile from Theoretical Calculations*, Acta Universitatis Upsaliensis, 2003.
15. W. Smith and T. Forester, *The DL_POLY Project*, TCS Division, Daresbury Laboratory, Daresbury, Warrington WA44AD, England.
16. R.W. Impey, P.A. Madden and I.R. McDonald, *J. Phys. Chem.*, **87** (1983) 5071.